BIOMOLECULES & THERAPEUTICS

Original Article
Biomol Ther 27(2), 222-230 (2019)

Vitamin D Improves Intestinal Barrier Function in Cirrhosis Rats by Upregulating Heme Oxygenase-1 Expression

Peng-fei Wang[1,†], Dan-hua Yao[1,†], Yue-yu Hu[2] and Yousheng Li[1,*]

[1]Department of General Surgery, Shanghai Ninth People's Hospital, Shanghai Jiaotong University School of Medicine, Shanghai 200011,
[2]Department of Neurology, The Fourth Affiliated Hospital of Tongji University, Shanghai 200081, China

Abstract

Intestinal barrier dysfunction always accompanies cirrhosis in patients with advanced liver disease and is an important contributor facilitating bacterial translocation (BT), which has been involved in the pathogenesis of cirrhosis and its complications. Several studies have demonstrated the protective effect of Vitamin D on intestinal barrier function. However, severe cholestasis leads to vitamin D depletion. This study was designed to test whether vitamin D therapy improves intestinal dysfunction in cirrhosis. Rats were subcutaneously injected with 50% sterile CCl_4 (a mixture of pure CCl_4 and olive oil, 0.3 mL/100 g) twice a week for 6 weeks. Next, $1,25(OH)_2D_3$ (0.5 μg/100 g) and the vehicle were administered simultaneously with CCl_4 to compare the extent of intestinal histologic damage, tight junction protein expression, intestinal barrier function, BT, intestinal proliferation, apoptosis, and enterocyte turnover. Intestinal heme oxygenase-1 (HO-1) expression and oxidative stress were also assessed. We found that vitamin D could maintain intestinal epithelial proliferation and turnover, inhibit intestinal epithelial apoptosis, alleviate structural damage, and prevent BT and intestinal barrier dysfunction. These were achieved partly through restoration of HO-1 and inhibition of oxidative stress. Taken together, our results suggest that vitamin D ameliorated intestinal epithelial turnover and improved the integrity and function of intestinal barrier in CCl_4-induced liver cirrhotic rats. HO-1 signaling activation was involved in these above beneficial effects.

Key Words: Bacterial translocation, Heme oxygenase-1, Vitamin D, Cirrhosis, Apoptosis, Proliferation

INTRODUCTION

Intestinal barrier dysfunction and bacterial translocation (BT) are common in patients with advanced liver disease, and there is strong evidence that gut-derived bacterial products play a central role in the onset of acute liver injury and progression to chronic liver disease (Wiest *et al*., 2014; Chazouilleres, 2016). In fact, many severe complications of cholestasis and cirrhosis are aggravated by BT including hepatic encephalopathy, hepatorenal syndrome, as well as hepato-cardiac syndrome (Alexopoulou *et al*., 2017; Piotrowski and Boron-Kaczmarska, 2017). This novel aspect of disease pathophysiology suggests that therapeutic strategies should aim at restoring the host intestinal mucosal barrier in cholestasis and cirrhosis.

Severe cholestasis leads to vitamin D depletion and vitamin D deficiency promotes cholestatic liver injury (Plourde *et al*., 1988; Firrincieli *et al*., 2013; Luger *et al*., 2016). The active form of vitamin D, $1,25(OH)_2D_3$, has an antiproliferative and antifibrotic effect on hepatic stellate cells and vitamin D inhibits its development of liver fibrosis in an animal model (Neeman *et al*., 2014; Abramovitch *et al*., 2015). However, the effect of vitamin D on intestinal barrier dysfunction in liver cholestasis has not been studied in detail. As a regulator of Toll-like receptor 4, vitamin D preserves intestinal epithelial barrier function and the vitamin D/vitamin D receptor (VDR) pathway has been shown to have intestinal protective effects in inflammatory bowel disease by inhibiting intestinal epithelial apoptosis (Barbalho *et al*., 2017; Shi *et al*., 2018). This study was designed to test whether vitamin D therapy improves intestinal dysfunction in cirrhosis.

Open Access **https://doi.org/10.4062/biomolther.2018.052**

Received Mar 21, 2018 **Revised** Jun 4, 2018 **Accepted** Jul 17, 2018
Published Online Sep 3, 2018

***Corresponding Author**
E-mail: lyswpf@gmail.com
Tel: +86-18019790260, Fax: +86-21-63136856.
[†]The first two authors contributed equally to this work.

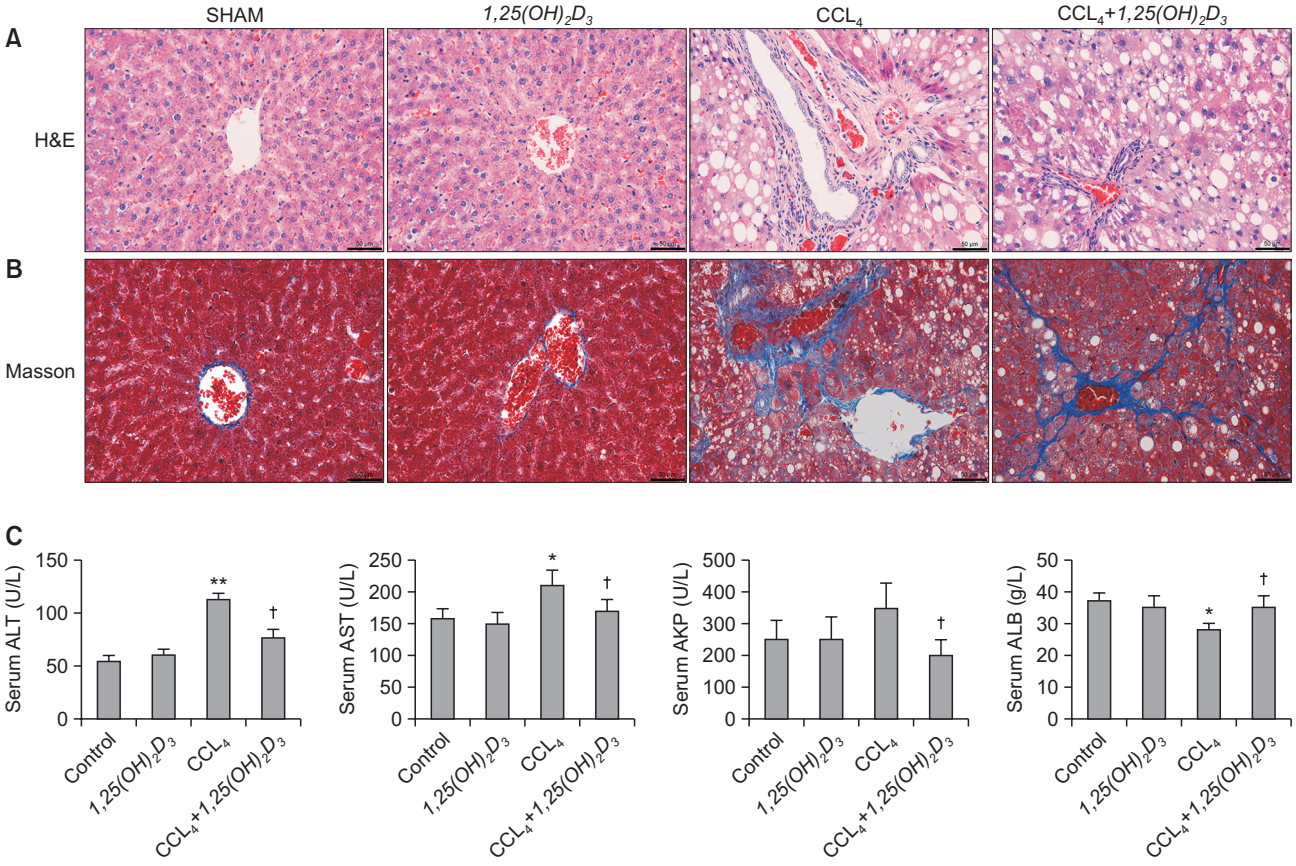

Fig. 1. *1,25(OH)$_2$D$_3$* improves liver function and fibrosis in CCl_4-treated rats. (A) Representative photomicrographs of liver histology (H&E) from each group. (B) Representative photomicrographs of liver histology (Masson's trichrome staining) from each group. (C) Levels of serum ALT, AST, AKP and ALB. **p*<0.05, vs. sham, ***p*<0.01, vs. sham. †*p*<0.05, vs. CCl4.

MATERIALS AND METHODS

Animals

Male Sprague-Dawley rats, weighing 200 to 250 g, were used in this study after 7 days of acclimatization. Rats were housed in an animal facility on a 12-h light/dark cycle, and were allowed access to standard rat chow and water ad libitum. All procedures were carried out in accordance with the "Principles of laboratory animal care" (NIH publication No. 85-23, revised 1985).

Liver fibrosis models

Liver fibrosis was induced by administering subcutaneous injections of sterile 50% CCl_4 (a mixture of pure CCl_4 and olive oil, 0.3 mL/100g body weight) twice a week for 10 weeks. *1,25(OH)$_2$D$_3$* (5 μg/mL), at a dose of 0.5 μg/100 g body weight, was injected simultaneously. A twice-weekly *1,25(OH)$_2$D$_3$* dosing regimen was chosen to prevent development of hypercalcemia (Abramovitch *et al*., 2015).

Animals were divided into the following four groups (n=8): the sham group, *1,25(OH)$_2$D$_3$* treatment group, CCl_4 treatment group, and combined treatment (CCl_4 and *1,25(OH)$_2$D$_3$*) group.

At the end of the treatment period, rats were anesthetized and blood samples were obtained by cardiac puncture. Samples of mesenteric lymph nodes (MLNs), liver, and spleen were also collected under sterile conditions and then the rats were euthanized. Distal ileum and colonic tissue samples were obtained and snap-frozen in liquid nitrogen for subsequent analysis. Other tissue samples were immediately fixed in 10% formalin for histochemical studies.

Table 1. Serum concentrations of 25-OH vitamin D

Group	*1,25(OH)$_2$D$_3$*
SHAM	49.4 ± 8.2
CCL4	36.3 ± 10.1*

**p*<0.05, vs. SHAM.

Biochemical assessment

Blood samples were centrifuged and serum was collected for alanine aminotransferase (ALT), aspartate aminotransferase (AST), alkaline phosphatase (AKP), and albumin (ALB) assay at a special clinical laboratory.

Bacterial translocation (BT)

Under sterile conditions, blood samples were cultured aerobically and anaerobically for 7 days. Samples of MLNs, liver, and spleen were placed in tubes containing thioglycolate broth

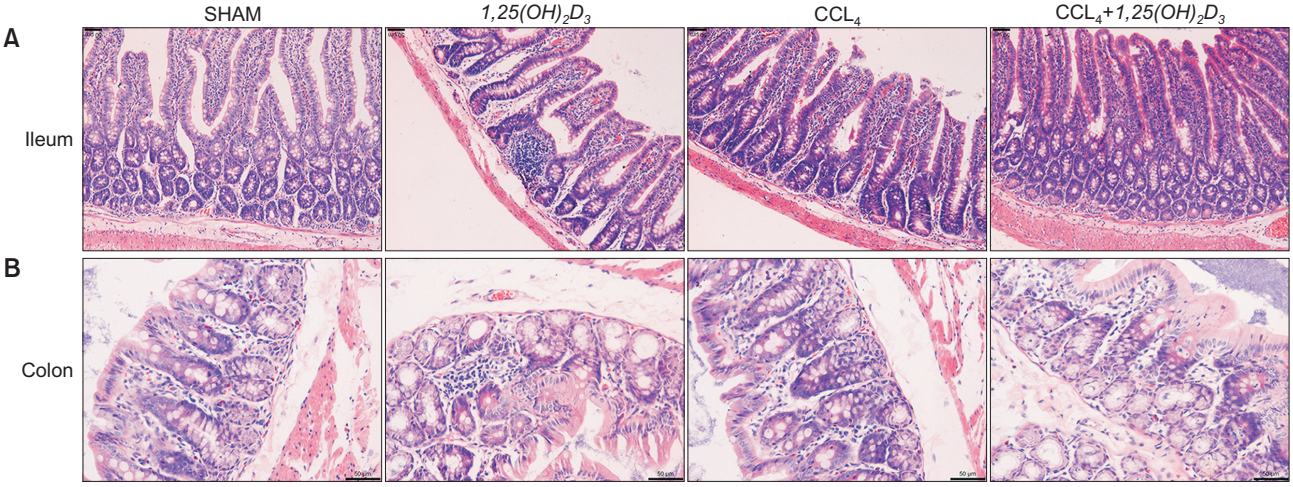

Fig. 2. *1,25(OH)$_2$D$_3$* maintains intestinal histologic integrity in CCl_4-treated rats. (A) Representative histological images (H&E staining) of intestine. (B) Representative histological images (H&E staining) of colon.

and homogenized and subjected to aerobic/anaerobic culture for 3 days. Bacterial growth was considered evidence of BT. The translocation ratio was calculated as the ratio of the total number of positive cultures of blood, MLNs, and organs to the total number of cultures of blood, MLNs, and organs tested in each group.

Histopathology

Histopathological examination was performed with light microscopy using 4 μm hematoxylin and eosin (H&E) stained tissue sections. Hepatic fibrosis was also evaluated with Masson Trichrome staining. Histopathological examinations were performed by a pathologist who was blinded to the study design.

Intestinal mucosal permeability

We used a modification of a previously reported method to assess intestinal mucosal permeability (Guttman, 2011). In this method, EZ-link® Sulfo-NHS-Biotin, molecular size 443 Da (Pierce Chemical Co., Rockford, IL, USA; Thermo Scientific Inc., Waltham, MA, USA) was used as a molecular tracer. In brief, a blunt-ended 18-gauge needle was gently inserted into the proximal colon that had been clamped using vessel cannulation forceps to grasp the needle through the colonic tissue. A sufficient amount of biotin tracer was injected into the lumen of the colon for 3.5 min to make it expand slightly. Following this, the region of colon in contact with the needle was removed (1 cm). The tissue was then washed three times in PBS and subjected to cryo-embedding, sectioning, and immunostaining by incubating with a 1:500 dilution of streptavidin conjugated to Alexa 488 (1:500; Molecular Probes, Eugene, OR, USA) for 30 min.

Intestinal permeability was also measured by fluorescein isothiocyanate (FITC)-dextran (FD-4)-based intestinal permeability methods as previously described (Gupta and Nebreda, 2014). A 5-cm segment of the ileal sac was ligated beginning at 3 cm proximal to the ileocecal valve, then PBS (pH 7.4) containing 25 mg/mL FD-4 was injected into the ileal sac to make it expand slightly. After 30 min, a blood sample (100 μL) was collected from the portal vein and immediately diluted with 1.9 mL of 50 mmol/L Tris (pH 10.3) containing 150 mmol/L sodium chloride. The diluted plasma was centrifuged at 3000 ×g for 10 min, and plasma FD-4 concentrations were determined using fluorescence spectrophotometry (ThermoFisher Scientific, Waltham, MA, USA) at an excitation wavelength of 480 nm and an emission wavelength of 520 nm.

Immunofluorescence

Sections of small intestinal and colonic tissue from all rats sacrificed for immunofluorescence staining were frozen in tissue freezing medium prior to cryo-embedding and sectioning. For immunostaining, 6 μm frozen sections were fixed in cold acetone for 15 min. Thereafter, tissues were permeabilized with 0.2% Triton X-100 in PBS for 20 min, and blocking was achieved by incubation with 5% goat serum. Incubation with primary antibodies ZO-1 (1:100; Zymed Laboratories Inc., San Francisco, CA, USA), occludin (1:200; Zymed Laboratories Inc.), heme oxygenase-1 (HO-1) (1:500; Abcam Inc., Cambridge, MA, USA) and proliferating cell nuclear antigen (PCNA) (1:500; Abcam Inc.) was performed overnight at 4°C. After three washes with PBS, the sections were incubated with Alexa 594-conjugated secondary antibodies (1:500; Molecular Probes) at room temperature for 2 h in the dark. Sections were then washed and mounted under coverslips using ProLong Gold antifade reagent with DAPI (Invitrogen, Carlsbad, CA, USA). The stained sections were visualized and photographed using a Nikon fluorescence microscope (NIS-Elements systems; Nikon Instruments Inc., Melville, NY, USA).

Epithelial proliferation and TUNEL assay

Crypt cell proliferation rate was calculated as the ratio of the number of crypt cells positive for PCNA labeling to the total number of crypt cells. The number of proliferating cells per crypt was defined as the mean of proliferating cells in 10 crypts (Cai *et al*., 2013). The terminal deoxynucleotidyl transferase (TdT)-mediated dUTP Nick-End Labeling (TUNEL) assay was used to detect fragmented DNA in situ on cryosections using an In Situ Cell Death Detection Kit-FITC (Roche Applied Science, Mannheim, Germany) and following the manufacturer's instructions. Double-labeling of TUNEL with PCNA was employed. For TUNEL assay, in each examina-

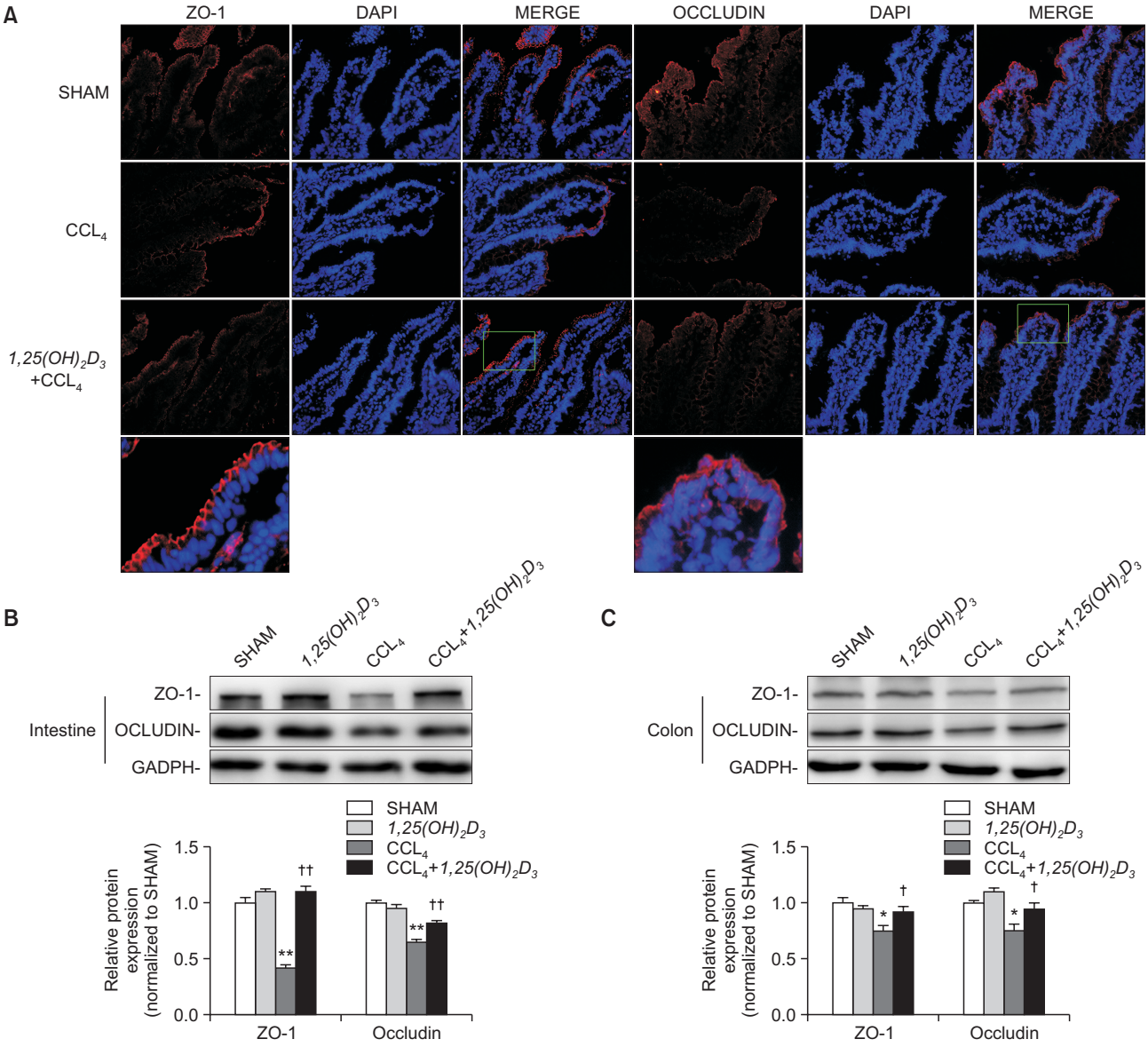

Fig. 3. *1,25(OH)$_2$D$_3$* maintains intestinal tight junction expression in CCl_4-treated rats. (A) ZO-1 and occludin expression in small bowel as determined by immunofluorescence (red), DAPI was used for nuclear labeling. Pictures highlighted in the green box are magnified below. (B) ZO-1 and occludin expression in small bowel as determined by western blot analysis. (C) ZO-1 and occludin expression in colon as determined by western blot analysis. Respective bands with GAPDH as loading control are shown at the bottom of the graphs. *p<0.05, vs. sham, **p<0.01, vs. sham. $^{\dagger}p$<0.05, vs. CCl_4, $^{\dagger\dagger}p$<0.01, vs. CCl_4.

tion, 1000 to 1500 cells from small intestinal villi without crypts were counted. Based on these observations, apoptotic index (AI) was defined as the count of positively stained cells in villi without crypts per 100 cells (Wang *et al*., 2010).

BrdU labeling and enterocyte migration

Standard 5-bromodeoxyuridine (BrdU) labeling reagent (Zymed Laboratories) was injected intraperitoneally at a dose of 50 mg/kg body weight 6 h before the animals were euthanized. Cell proliferation was assessed using biotinylated sheep polyclonal anti-BrdU antibody (1:500; Abcam Inc.). For ease of assessment, the villus was divided into base, middle, and top parts. Quantification of BrdU+ cells along the crypt–villus axis was performed.

Western blotting

Frozen biopsies were disrupted with a tissue lyser in radioimmunoprecipitation assay buffer, and total protein was quantified using the bicinchoninic acid (BCA) method. Equal concentration of proteins was loaded into a 6-10% sodium dodecyl sulfate-polyacrylamide gel and then electrotransferred. Membranes were blocked, incubated with the corresponding primary antibody at 4°C overnight, and then incubated with horseradish peroxidase-conjugated goat anti-rabbit IgG antibody (1:20000; Sigma-Aldrich, St. Louis, MO, USA) for 1 h at room temperature. After washing, the immune complexes

were detected using ECL detection reagent (Pierce Chemical Co., Thermo Scientific). Primary antibodies used for western blotting were: ZO-1, occludin, HO-1, GADPH (1:1000; CST Inc., Cell Signaling Technology, Danvers, MA, USA). Protein expression of each molecule was expressed as relative intensity and normalized to GADPH.

Oxidative stress measurement

Protein concentration of tissues was assayed using a BCA assay kit from (Bio-Rad Laboratories, Inc., Hercules, CA, USA). Lipid peroxidation was evaluated by measuring the production of malondialdehyde (MDA) with a lipid peroxidation MDA assay kit (Beyotime, Shanghai, China). Glutathione (GSH) was assayed by using the spectrophotometric method, which is based on the use of Ellman's reagent.

Statistical analysis

Data are reported as the mean ± 1.0 SD when appropriate. Differences in BT occurrence between groups were compared by using Fisher's exact test. Differences between means were evaluated by one-way ANOVA test. Bonferroni test was applied for pairwise comparison of every combination of group pairs. All analyses were conducted in SPSS13.0 software (SPSS Inc., Chicago, IL, USA). Statistical significance was set at $p<0.05$.

RESULTS

Effect of *1,25(OH)$_2$D$_3$* on CCl_4-induced hepatotoxicity

HE-staining showed that control rats showed no pathological changes in the liver. Liver tissues in the CCl_4 group showed degenerative changes and centrilobular necrosis; hepatocytes showed ballooning, lipid droplet deposition, and inflammatory cell infiltration, as well as collagen deposition (Fig. 1A). Obvious bridging fibrosis was also observed in the CCl_4 group, which showed periportal collagen deposition and staggered fibrosis formation, forming a large number of false lobules (Fig. 1B). However, pathological liver damage and fibrosis were mildly diminished in *1,25(OH)$_2$D$_3$*-treated animals.

The levels of serum ALT, AST, and AKP were higher in CCl_4-treated rats, while ALB levels were lower. In *1,25(OH)$_2$D$_3$*-treated animals, serum ALT, AST, and AKP levels decreased compared with CCl_4-treated animals; ALB levels however were increased (Fig. 1C). Additionally, serum 25-OH vitamin D concentrations were significantly lower ($p<0.05$) in the CCl_4 group compared with the sham group (Table 1).

Effect of *1,25(OH)$_2$D$_3$* on intestinal histologic damage in cirrhosis

HE staining shows that villous height was homogenously distributed with minimal inflammatory cell infiltration in sham rats (Fig. 2A, 2B). In CCl_4-treated rats, ileal lymphangiectasia, submucosal cecal edema, and significant inflammatory cell infiltration were observed. However, the intestinal villi of the rats treated with *1,25(OH)$_2$D$_3$* were more uniform and inflammatory cell infiltration was absent.

Effect of *1,25(OH)$_2$D$_3$* on intestinal tight junction protein expression

In line with the altered intestinal histologic damage, we demonstrated the effects of *1,25(OH)$_2$D$_3$* on tight junction protein expression. As illustrated in Fig. 3, western blot analysis and immunofluorescence indicated that *1,25(OH)$_2$D$_3$* treatment abrogated the CCl_4-induced loss of ZO-1 and occludin expression in the villi.

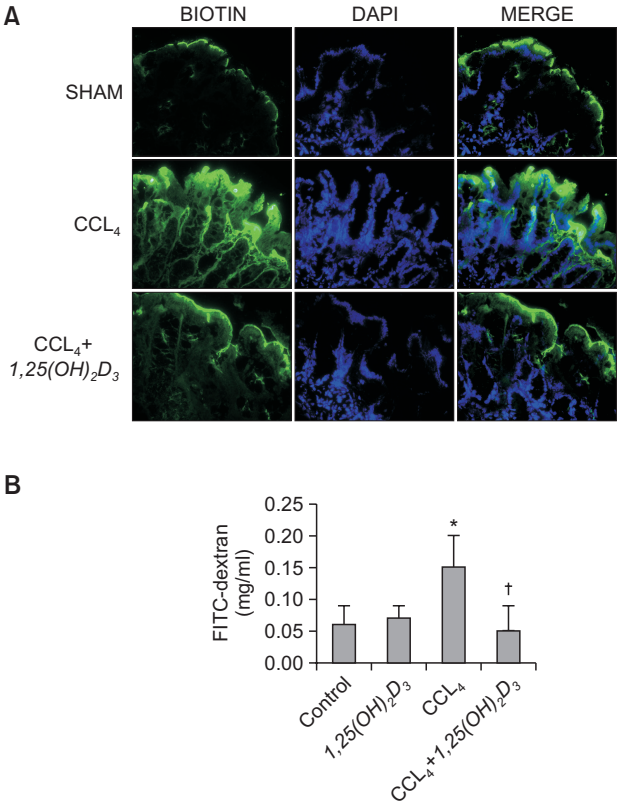

Fig. 4. *1,25(OH)$_2$D$_3$* maintains intestinal permeability in CCl_4 treated rats. (A) Colonic tissues were stained with the molecular tracer biotin to examine barrier permeability. DAPI was used for nuclear labeling. (B) Effects of *1,25(OH)$_2$D$_3$* on intestinal permeability as measured by FITC-dextran (FD-4)-based intestinal permeability methods. *$p<0.05$, vs. sham, †$p<0.05$, vs. CCl_4.

Effect of *1,25(OH)$_2$D$_3$* on intestinal permeability and BT

To determine whether the altered distribution of tight junction proteins induced functional disruption, we utilized biotin as a molecular tracer to assess the integrity of the epithelial barrier. Biotin was found to be restricted solely to the luminal boundary of the colon epithelium in the sham group (Fig. 4A). In CCl_4-treated rats, biotin was no longer restricted to the luminal bounder but had permeated the epithelium and extended into the lamina propria. However, the effect was inhibited by treatment with *1,25(OH)$_2$D$_3$*. *In vivo*, plasma levels of FD4 in CCl_4-treated rats were significantly increased relative to sham-treated controls. Rats treated with *1,25(OH)$_2$D$_3$* also displayed a significant reduction in leakage of FD4 across the intestinal wall compared with the CCl_4 group (Fig. 4B).

No bacteria was detected in the blood of rats in all groups. BT to MLNs was observed in the sham group. However, the occurrence of BT was increased in MLNs, liver, spleen, and kidney of the CCl_4-treated rats compared with those of the sham group. *1,25(OH)$_2$D$_3$* treatment reduced the occurrence of BT during the development of liver cirrhosis in group

Table 2. Growth of bacterial from harvested samples

Group	MLN+	Liver+	Slpeen+	Kidney+	Blood+	TR
SHAM	2/8	0/8	0/8	0/8	0/8	5%
SHAM+*1,25(OH)$_2$D$_3$*	1/8	0/8	0/8	1/8	0/8	5%
CCL_4	8/8**	3/8	2/8	4/8	0/8	42.5%**
CCL_4+*1,25(OH)$_2$D$_3$*	4/8$^{\&}$	2/8	1/8	2/8	0/8	22.5%$^{\&}$

+indicates bacterial growth which was considered as evidence of BT.
*p<0.05, vs. SHAM, **p<0.01, vs. SHAM. $^{\&}p$<0.05, vs. CCL4.

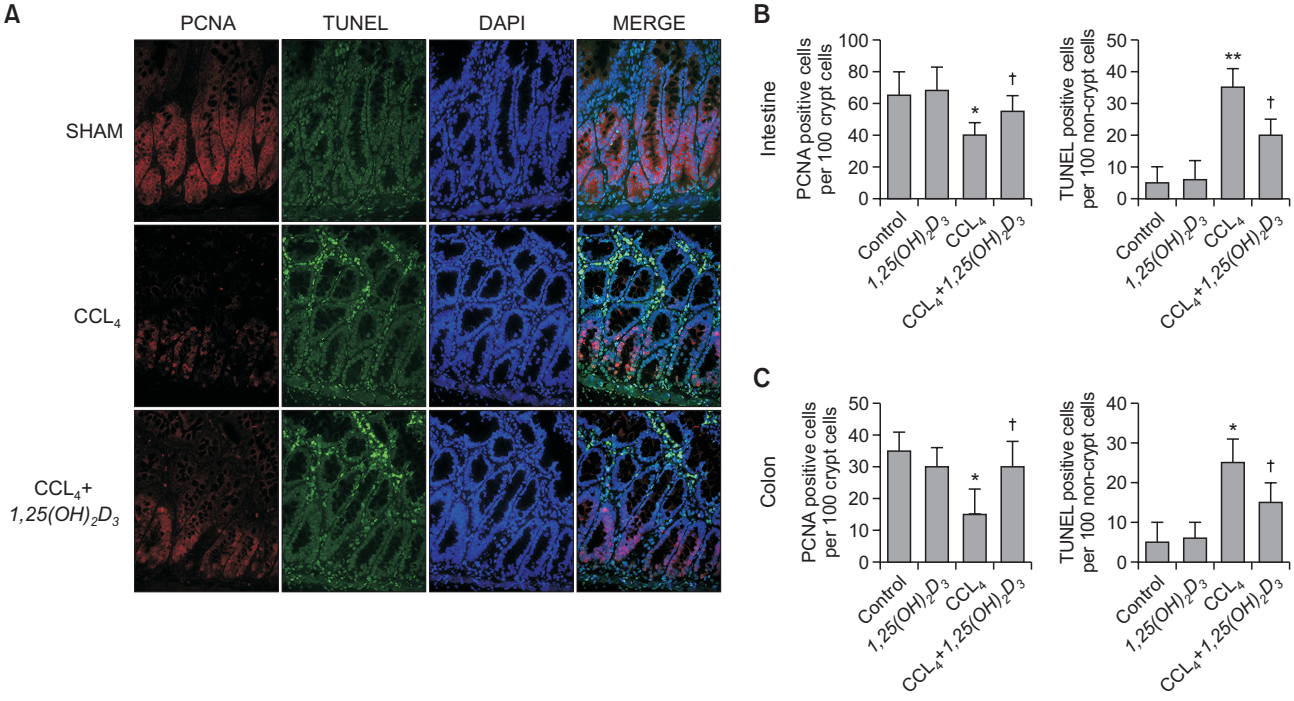

Fig. 5. *1,25(OH)$_2$D$_3$* maintains intestinal proliferation, apoptosis, and enterocyte turnover in CCl4-treated rats. (A) TUNEL (blue) assay with PCNA double-labeling (red) in small bowel as determined by immunofluorescence; DAPI was used for nuclear labeling. (B) Crypt cell proliferation rate and apoptotic index (AI) in small intestine. (C) Crypt cell proliferation rate and apoptotic index (AI) in colon. *p<0.05, vs. sham, **p<0.01, vs. sham. $^{\dagger}p$<0.05, vs. CCl_4.

CCl_4+*1,25(OH)$_2$D$_3$*-treated rats (Table 2).

Effect of *1,25(OH)$_2$D$_3$* on intestinal proliferation, apoptosis, and enterocyte turnover

We hypothesized that disequilibrium between proliferation and apoptosis in intestinal epithelial cells would result in intestinal barrier dysfunction. The VDR pathway has been shown to have intestinal protective effects via inhibiting intestinal epithelial apoptosis (Barbalho *et al*., 2017; Shi *et al*., 2018). We demonstrated the effects of *1,25(OH)$_2$D$_3$* on intestinal proliferation and apoptosis. The activity of *1,25(OH)$_2$D$_3$* on the proliferation of intestinal cells in mice treated with CCl_4 was observed by using immunofluorescence of PCNA labeling as well as TUNEL and PCNA double-labeling.

As illustrated in Fig. 5A, immunofluorescence indicated that CCl_4 treatment hampered cell proliferation in the small intestinal crypts, and the proliferating crypt cells in CCl_4-treated rats were shown to be scattered and in disarray. However, *1,25(OH)$_2$D$_3$* administration restored the proliferative ability of crypt cells in both small intestines and colon (Fig. 5B, 5C). Meanwhile, we found a markedly greater number of apoptotic cells in the intestinal epithelium of the CCl_4-treated group than in the sham group, but this was significantly ameliorated by *1,25(OH)$_2$D$_3$* administration.

Enterocyte migration indicated by BrdU immunopositive cells was found within the basal and middle zone 6 h after BrdU injection (Fig. 6A). A statistically significant decrease in cell migration was detected in CCl_4-treated rats, while *1,25(OH)$_2$D$_3$* administration maintained intestinal epithelial turnover at normal levels (Fig. 6B).

Effect of *1,25(OH)$_2$D$_3$* on intestinal HO-1 expression and oxidative stress

HO-1 can be induced by inflammatory cytokines, oxidation, ischemia, hypoxia, and endotoxins (Loboda *et al*., 2016). Over-expression of HO-1 promotes intestinal epithelial cell

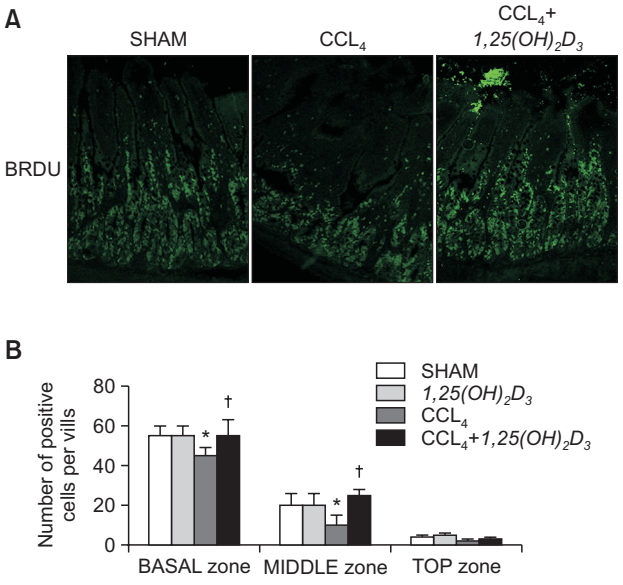

Fig. 6. *1,25(OH)$_2$D$_3$* maintains enterocyte turnover in CCl_4-treated rats. (A) BrdU expression in small intestine 6 h after BrdU injection. (B) Quantification of BrdU+ cells along the crypt-villus axis. *p<0.05, vs. sham. †p<0.05, vs. CCl_4.

proliferation and migration (Zhang *et al*., 2013a). So, we investigated whether the VDR pathway ameliorates intestinal dysfunction by regulating HO-1. HO-1 expression increased slightly in intestinal tissue of CCl_4-treated rats, but was significantly upregulated by *1,25(OH)$_2$D$_3$* (Fig. 7A, 7B). HO-1 and its products exert beneficial effects through protection against oxidative injury, subsequently regulating apoptosis and inflammation. We further studied the effect of *1,25(OH)$_2$D$_3$* on intestinal oxidative stress (Fig. 7C-7F).

MDA levels were monitored to evaluate the effect of *1,25(OH)$_2$D$_3$* treatment on CCl_4-induced intestinal lipid peroxidation. MDA levels in the CCl_4 group were significantly higher than those in the sham group. *1,25(OH)$_2$D$_3$* treatment is known to significantly decrease MDA levels and GSH plays pivotal roles in free radical scavenging and prevention of reactive oxygen species-induced liver damage. GSH levels in the CCl_4 group were lower than those in the sham group, and GSH levels in the *1,25(OH)$_2$D$_3$* group were higher than those in the CCl_4 group.

DISCUSSION

In this study, we found that proliferation and apoptosis of intestinal epithelial cells play critical roles in cirrhosis-associated intestinal mucosal barrier dysfunction. Our results showed that *1,25(OH)$_2$D$_3$* restored the proliferative ability of crypt cells in the intestines, inhibited enterocyte apoptosis, maintained normal intestinal epithelial turnover, and improved the integrity and function of the intestinal epithelial barrier in CCl_4-induced liver cirrhotic rats. These beneficial effects can be ascribed, at least in part, to the effect of activation of *1,25(OH)$_2$D$_3$* on the HO-1 signaling pathway.

BT has been studied in animals subjected to various pathological conditions such as hemorrhagic shock, sepsis, intestinal obstruction, inflammatory bowel disease, acute pancreatitis, and total parenteral nutrition (Nagpal and Yadav, 2017). Intestinal barrier dysfunction is always associated with cirrhosis and is an important contributor facilitating BT, which has been involved in the pathogenesis of cirrhosis and its complications (Wiest *et al*., 2014; Chazouilleres, 2016; Alexopoulou *et al*., 2017; Piotrowski and Boron-Kaczmarska, 2017). Consistent with previous studies, our findings showed that significant intestinal morphological alterations and tight junction protein loss occurred in CCl_4-induced liver cirrhotic rats (Chen *et al*., 2016). Interestingly, ZO-1 and occludin were highly expressed in small bowel than in the colon of the CCl_4 group. This was different from findings from a previous study and may be related to differing periods of observation (Fouts *et al*., 2012). To determine whether the altered distribution of tight junction proteins induced functional disruption, we also utilized biotin as a molecular tracer to assess the integrity of the epithelial barrier. Biotin permeated the epithelium and extended into the lamina propria. Correspondingly, BT was increased in MLNs, liver, spleen, and kidney in CCl_4-induced liver cirrhotic rats. However, the above effects were inhibited following treatment with *1,25(OH)$_2$D$_3$*.

The protective effects of vitamin D have been demonstrated in many organs and tissues besides the gut (Zhang *et al*., 2013b). Severe cholestasis leads to vitamin D depletion and vitamin D deficiency promotes cholestatic liver injury (Plourde *et al*., 1988; Firrincieli *et al*., 2013; Luger *et al*., 2016). *1,25(OH)$_2$D$_3$*, the active form of vitamin D, has an antiproliferative and antifibrotic effect on hepatic stellate cells and vitamin D inhibited development of liver fibrosis in an animal model (Neeman *et al*., 2014; Abramovitch *et al*., 2015). However, the underlying mechanism is not clear. Oxidative stress has been considered to be a major factor in the pathogenesis of hepatic fibrosis (Rocha *et al*., 2014). A recent study indicated that vitamin D appears to act as an antioxidant to protect the rat liver against damage (Ozerkan *et al*., 2017). In the present study, we confirmed that *1,25(OH)$_2$D$_3$* treatment also significantly improved intestinal oxidative injury. HO-1, as an Nrf2-dependent gene, exerts beneficial effects through protection against oxidative injury (Loboda *et al*., 2016). In our study, HO-1 expression was significantly diminished in intestinal tissue of CCl_4-treated rats, but this was reversed by treatment with *1,25(OH)$_2$D$_3$*. It is worth noting that, regulation of microbial function as well as oxidative stress might both be similarly important targets in the treatment of liver fibrosis and cirrhosis. BT and immune dysfunction have been involved in the pathogenesis of cirrhosis and its complications (Wiest *et al*., 2014; Chazouilleres, 2016). Our findings suggest that improved intestinal barrier function and diminished BT might contribute to the antifibrotic effect of vitamin D.

The integrity of the intestinal mucosal barrier depends on the balance between epithelial cell proliferation and apoptosis. Strategies to protect mainly the intestinal mucosal barrier could attenuate apoptosis and maintain the proliferative ability of intestinal crypt cells. Our study revealed a significant decrease in cell migration detected in CCl_4-treated rats; however, *1,25(OH)$_2$D$_3$* administration maintained intestinal epithelial turnover at normal levels. Accumulating evidence suggests that overexpression of HO-1 promotes intestinal epithelial cell proliferation and migration (Uc and Britigan, 2003; Zhang *et al*., 2013a). So, it is speculated that down-regulation of HO-1 is involved in the inhibition of intestinal epithelial proliferation

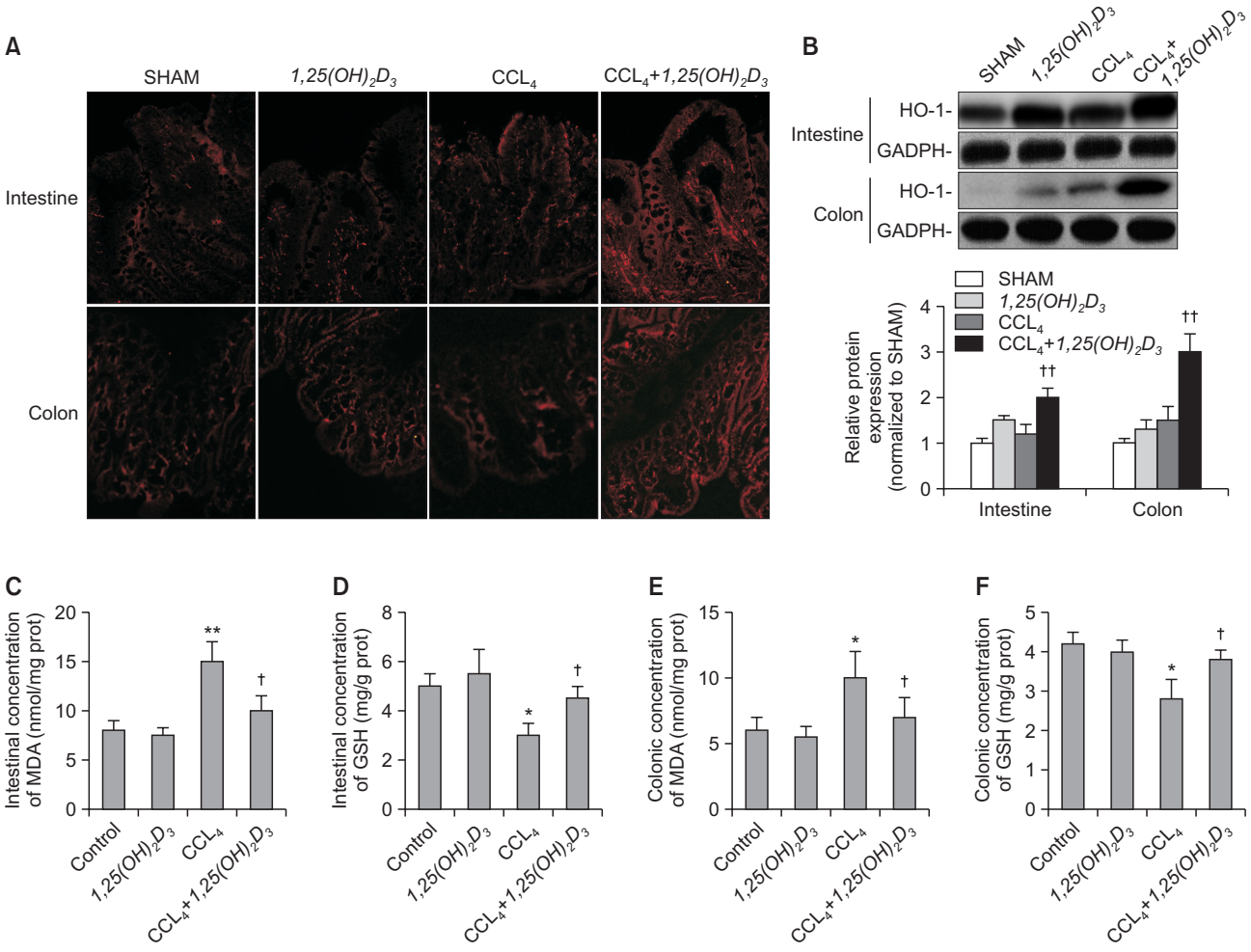

Fig. 7. *1,25(OH)$_2$D$_3$* maintains intestinal HO-1 expression and inhibits oxidative stress in CCl_4-treated rats. (A) HO-1 expression in small bowel and colon as determined by immunofluorescence. (B) HO-1 expression in small bowel and colon as determined by western blot analysis. Respective bands with GAPDH as loading control are shown at the bottom of the graphs. (C-F) MDA levels and GSH levels in small bowel and colon; *p<0.05, vs. sham, **p<0.01, vs. sham. $^{\dagger}p$<0.05, vs. CCl_4, $^{\dagger\dagger}p$<0.01 vs. CCl_4.

and the apoptosis that occurs with cirrhosis, while *1,25(OH)$_2$D$_3$* administration induces HO-1 activation and accelerates intestinal epithelial turnover.

The present study has several limitations. Mainly, the assessment of the function of HO-1 and the analysis of loss of inflammation. Although we have observed that HO-1 is involved in intestinal barrier dysfunction in cirrhotic rats, advanced experiments involving HO-1 inhibition or silence are important and can directly elucidate the underlying mechanism.

In conclusion, *1,25(OH)$_2$D$_3$* has shown significant protective effects in ameliorating intestinal barrier dysfunction in CCl_4-induced cirrhotic rats. This beneficial effect is chiefly ascribed to its effect on maintenance of intestinal epithelial proliferation and turnover, probably via activation of the HO-1-mediated signaling pathway. Thus, *1,25(OH)$_2$D$_3$* may represent a new therapeutic agent useful for protection against cirrhosis-associated intestinal barrier dysfunction.

ACKNOWLEDGMENTS

This work is supported by National Natural Science Foundation of China projects 81100249 (to Peng-fei Wang) and 81301610 (to Yue-yu Hu). There is no potential conflict of interest involved in this paper.

REFERENCES

Abramovitch, S., Sharvit, E., Weisman, Y., Bentov, A., Brazowski, E., Cohen, G., Volovelsky, O. and Reif, S. (2015) Vitamin D inhibits development of liver fibrosis in an animal model but cannot ameliorate established cirrhosis. *Am. J. Physiol. Gastrointest. Liver Physiol.* **308**, G112-G120.

Alexopoulou, A., Agiasotelli, D., Vasilieva, L. E. and Dourakis, S. P. (2017) Bacterial translocation markers in liver cirrhosis. *Ann. Gastroenterol.* **30**, 486-497.

Barbalho, S. M., Goulart, R. A. and Gasparini, R. G. (2017) Associations between inflammatory bowel diseases and vitamin D. *Crit. Rev. Food Sci. Nutr.* doi: 10.1080/10408398.2017.1406333 [Epub ahead of print].

Cai, Y., Wang, W., Liang, H., Sun, L., Teitelbaum, D. H. and Yang, H. (2013) Keratinocyte growth factor pretreatment prevents radiation-induced intestinal damage in a mouse model. *Scand. J. Gastroenterol.* **48**, 419-426.

Chazouilleres, O. (2016) Novel aspects in the management of cholestatic liver diseases. *Dig. Dis.* **34**, 340-346.

Chen, Y. X., Lai, L. N., Zhang, H. Y., Bi, Y. H., Meng, L., Li, X. J., Tian, X. X., Wang, L. M., Fan, Y. M., Zhao, Z. F., Han, D. W. and Ji, C. (2016) Effect of artesunate supplementation on bacterial translocation and dysbiosis of gut microbiota in rats with liver cirrhosis. *World J. Gastroenterol.* **22**, 2949-2959.

Firrincieli, D., Zuniga, S., Rey, C., Wendum, D., Lasnier, E., Rainteau, D., Braescu, T., Falguieres, T., Boissan, M., Cadoret, A., Housset, C. and Chignard, N. (2013) Vitamin D nuclear receptor deficiency promotes cholestatic liver injury by disruption of biliary epithelial cell junctions in mice. *Hepatology* **58**, 1401-1412.

Fouts, D. E., Torralba, M., Nelson, K. E., Brenner, D. A. and Schnabl, B. (2012) Bacterial translocation and changes in the intestinal microbiome in mouse models of liver disease. *J. Hepatol.* **56**, 1283-1292.

Gupta, J. and Nebreda, A. (2014) Analysis of intestinal permeability in mice. *Bio-protocol* **4**, e1289.

Guttman, J. A. (2011) Using molecular tracers to assess the integrity of the intestinal epithelial barrier *in vivo*. *Methods Mol. Biol.* **762**, 275-280.

Loboda, A., Damulewicz, M., Pyza, E., Jozkowicz, A. and Dulak, J. (2016) Role of Nrf2/HO-1 system in development, oxidative stress response and diseases: an evolutionarily conserved mechanism. *Cell. Mol. Life Sci.* **73**, 3221-3247.

Luger, M., Kruschitz, R., Kienbacher, C., Traussnigg, S., Langer, F. B., Schindler, K., Wurger, T., Wrba, F., Trauner, M., Prager, G. and Ludvik, B. (2016) Prevalence of liver fibrosis and its association with non-invasive fibrosis and metabolic markers in morbidly obese patients with vitamin D deficiency. *Obes. Surg.* **26**, 2425-2432.

Nagpal, R. and Yadav, H. (2017) Bacterial translocation from the gut to the distant organs: an overview. *Ann. Nutr. Metab.* **71 Suppl 1**, 11-16.

Neeman, R., Abramovitch, S., Sharvit, E., Elad-Sfadia, G., Haklai, R., Kloog, Y. and Reif, S. (2014) Vitamin D and S-farnesylthiosalicylic acid have a synergistic effect on hepatic stellate cells proliferation. *Dig. Dis. Sci.* **59**, 2462-2469.

Ozerkan, D., Ozsoy, N., Akbulut, K. G., Guney, S. and Ozturk, G. (2017) The protective effect of vitamin D against carbon tetrachloride damage to the rat liver. *Biotech. Histochem.* **92**, 513-523.

Piotrowski, D. and Boron-Kaczmarska, A. (2017) Bacterial infections and hepatic encephalopathy in liver cirrhosis-prophylaxis and treatment. *Adv. Med. Sci.* **62**, 345-356.

Plourde, V., Gascon-Barré, M., Willems, B. and Huet, P. M. (1988) Severe cholestasis leads to vitamin D depletion without perturbing its C-25 hydroxylation in the dog. *Hepatology* **8**, 1577-1585.

Rocha, S. W., de Franca, M. E., Rodrigues, G. B., Barbosa, K. P., Nunes, A. K., Pastor, A. F., Oliveira, A. G., Oliveira, W. H., Luna, R. L. and Peixoto, C. A. (2014) Diethylcarbamazine reduces chronic inflammation and fibrosis in carbon tetrachloride- (CCl(4)-) induced liver injury in mice. *Mediators Inflamm.* **2014**, 696383.

Shi, Y., Liu, T., Zhao, X., Yao, L., Hou, A., Fu, J. and Xue, X. (2018) Vitamin D ameliorates neonatal necrotizing enterocolitis via suppressing TLR4 in a murine model. *Pediatr. Res.* **83**, 1024-1030.

Uc, A. and Britigan, B. E. (2003) Does heme oxygenase-1 have a role in Caco-2 cell cycle progression? *Exp. Biol. Med. (Maywood)* **228**, 590-595.

Wang, P., Gong, G., Wei, Z. and Li, Y. (2010) Ethyl pyruvate prevents intestinal inflammatory response and oxidative stress in a rat model of extrahepatic cholestasis. *J. Surg. Res.* **160**, 228-235.

Wiest, R., Lawson, M. and Geuking, M. (2014) Pathological bacterial translocation in liver cirrhosis. *J. Hepatol.* **60**, 197-209.

Zhang, L., Liu, Y. L., Chen, G. X., Cui, B., Wang, J. S., Shi, Y. L., Li, L. P. and Guo, X. B. (2013a) Heme oxygenase-1 promotes Caco-2 cell proliferation and migration by targeting CTNND1. *Chin. Med. J.* **126**, 3057-3063.

Zhang, Y. G., Wu, S. and Sun, J. (2013b) Vitamin D, vitamin D receptor, and tissue barriers. *Tissue Barriers* **1**, e23118.